ACS APPLIED MATERIALS & INTERFACES

Letter

www.acsami.org

Direct Observation of Nanoscale Pt Electrode Agglomeration at the Triple Phase Boundary

Chen-Chiang Yu,[†,‡,§] Sanwi Kim,[†,⊥] Jong Dae Baek,[‡] Yong Li,[‡] Pei-Chen Su,*[,‡] and Taek-Soo Kim*[,⊥]

[‡]School of Mechanical & Aerospace Engineering, Nanyang Technological University, 50 Nanyang Avenue 639798, Singapore

[§]Energy Research Institute @ NTU, Interdisciplinary Graduate School, Nanyang Technological University, 50 Nanyang Avenue 639798, Singapore

[⊥]Department of Mechanical Engineering, Korea Advanced Institute of Science and Technology, 291 Daehak-ro Yuseong-gu, Daejeon 305-701, South Korea

Supporting Information

ABSTRACT: Nanoporous platinum electrode thin films were delaminated from yttria-stabilized zirconia (YSZ) substrates via double cantilever beam delamination to reveal the structure located at the interface between electrode and electrolyte. The thermally driven morphological evolution between the electrode top surface and the substrate contact interface of agglomerated nanoporous platinum thin films were compared. We found the temperature required for significant agglomeration to occur was approximately 100 °C higher at the electrolyte contact interface side than at the top surface side. Judging the reaction active site from the electrode top surface could be inaccurate because higher resistance of thermal agglomeration at the interface could retain the reaction active site during fuel cell operation.

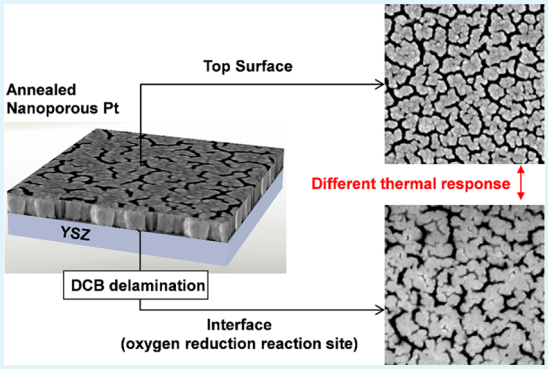

KEYWORDS: *nanoporous Pt electrode agglomeration, yttria-stabilized zirconia (YSZ), fuel cell, layer delamination, triple phase boundary (TPB)*

Nanoporous platinum thin films deposited on yttria-stabilized zirconia (YSZ) substrates as cathodes for oxygen reduction reaction (ORR) have important applications in miniature solid-state electrochemical devices, such as oxygen sensors and micro solid oxide fuel cells (μ-SOFCs).[1,2] μ-SOFCs use a combination of nanoscale thin film components including a freestanding YSZ electrolyte membrane and two porous thin film electrodes that sandwich the YSZ electrolyte. Because the thickness of the electrolyte is significantly minimized, the ohmic resistance of ion/proton transportation is also significantly reduced; therefore, a good device performance even at very low temperatures is possible.[3−5]

For μ-SOFCs operated at temperatures below 500 °C, the sluggish ORR at the cathode becomes the most rate-limiting process. The oxygen incorporation from the Pt electrode into the YSZ electrolyte at the vicinity of the Pt/YSZ/O_2 junctions (or the triple phase boundaries, TPBs) is believed to be one of the slowest ORR steps.[6] Because the interface between the Pt thin-film electrode and YSZ electrolyte is two-dimensional, the effective TPBs for ORRs are only located at the Pt pore boundaries on the surface of the YSZ substrate (i.e., TPBs). Therefore, a high density of TPB sites at the Pt/YSZ contact interface is critical in order to obtain high device performance.

The platinum electrode thin films for μ-SOFCs are usually deposited on YSZ via sputtering at high Ar pressure and low DC power in order to generate a high density of nanoscale pores within the film,[7] and the resulting pore sizes are in the range of a few to tens of nanometers.[8] These nanoscale pores are poor in maintaining thermal stability, which inevitably results in decreased TPB densities. Therefore, knowing precisely the microstructural morphology of porous Pt electrodes at the Pt/YSZ contact interface and how the morphology evolves with increasing operating temperatures will provide important information to engineer the nanostructure of electrodes with better thermal stability.

The observation of thermally driven morphological evolution of micrometer-scale pores in Pt thin film electrodes is not new,[8−12] but the observation of nanoscale pores is rare. In these studies, Pt electrodes with micrometer pores were prepared via depositing a thick and dense film, followed by thermal annealing at very high temperatures (650−800 °C) to generate micrometer-scale pores (Figure 1a). The TPB densities were then estimated by counting the line density of the pore perimeters in an SEM image of the electrode "top view",[13] and the dense part of the film is assumed to have little or no contribution to the effective TPB sites because the oxygen bulk diffusion through Pt is insignificant compared with the oxygen surface diffusion. For Pt thin film electrodes with micrometer-

Received: January 8, 2015
Accepted: March 10, 2015
Published: March 10, 2015

DOI: 10.1021/acsami.5b00134
ACS Appl. Mater. Interfaces 2015, 7, 6036−6040

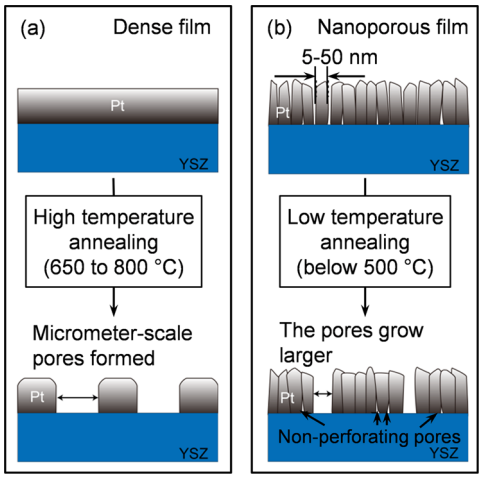

Figure 1. Different ways of porous Pt thin film preparation results in different scale of pore-size and different film structure during TPB study: (a) The Pt electrode is first deposited as a dense film followed by high temperature annealing to generate pores in the thin film. The pore formed is micrometer-scale and perforated. (b) Porous Pt thin film is deposited directly with nanometer-scale pores and treated at the lower temperatures to study morphological evolution. There are nonperforation pores hiding beneath.

scale pores, relatively low TPB densities of only few micrometers per unit area (μm^{-1}) were shown.[9,10] However, such estimation of TPB from electrode top view have been undertaken with the assumption that the morphology at the top surface is identical to that at the Pt/YSZ contact interface, which is only valid if all the pores are through-holes across the electrode thickness.

On the other hand, the Pt electrodes for the application of μ-SOFCs have pores in nanometers to tens of nanometers scale and are typically deposited directly as "porous" films. A very high density of nanoscale features, such as nanocracks, nanopores, and grain boundaries within the Pt electrode thin film, and a high density of effective TPB in the range of tens of micrometers per unit area (μm^{-1}) is usually obtained. However, these nanoscale features can be nonperforating through the electrode film and are therefore not visible from electrode top view, but still function as effective TPB sites (Figure 1b). In this case, the estimation results of TPB densities by viewing the top morphology of the electrode can no longer represent the actual microstructural contacts at the Pt/YSZ interface that contribute to the effective TPBs. Recently, Ryll et al. reported a significant contribution of the effective TPB within a apparently dense electrode with thicknesses of 15−360 nm.[10] They compared the impedance data between two dense electrodes and proposed the existence of "nanoscopic" TPBs (e.g., grain boundaries, invisible cracks, or combinations thereof) that are not visible from the electrode's top surface but are oxygen-permeable and can function as effective ORR sites. However, it is likely that the dense films prepared by Ryll et al. in their experiments were not completely dense and actually contain a high density of nanoscale features that were not visible from the electrode top surface. From their cross-sectional view and tilted backside view of a thin film Pt electrode, nanoscale cracks seemed to exist under the dense films, but a clear image was not available in their results.

The thermal agglomeration behavior between the electrode top and YSZ interface is expected to be different because the unbounded surface Pt is free to migrate under the effect of heat, whereas the bonded interfacial Pt to the YSZ substrate is constraint to migrate. However, the information on how different is such behavior between the two sides of the electrode remains lacking. Therefore, to obtain information on the Pt morphology at the Pt/YSZ interface is necessary for μ-SOFCs using porous Pt as electrodes. It is important to accurately identify the critical temperature at which the nanoscopic TPB density significantly decreases in order to determine the highest suitable operating temperature for such a device.

In this work, the necessity of the direct electrode morphology observations of the nanoscale pores for these two-dimensional TPB systems at the Pt/YSZ interface is demonstrated. A delamination method based on double cantilever beam (DCB) technique is applied to neatly delaminate the porous Pt thin film from YSZ substrate in order to reveal the hidden interfacial morphology of Pt. DCB technique allows precise control of delamination up to atomic-thin monolayer along the targeted interface.[14,15] Because the load applied during the delamination is in the normal direction to the crack plane (mode I loading), the porous Pt thin film is only delaminated by out-of-plane movements and it does not experience shear forces. Therefore, the original interfacial morphology at the Pt/YSZ interface can be preserved after delamination. With the help of DCB delamination technique,

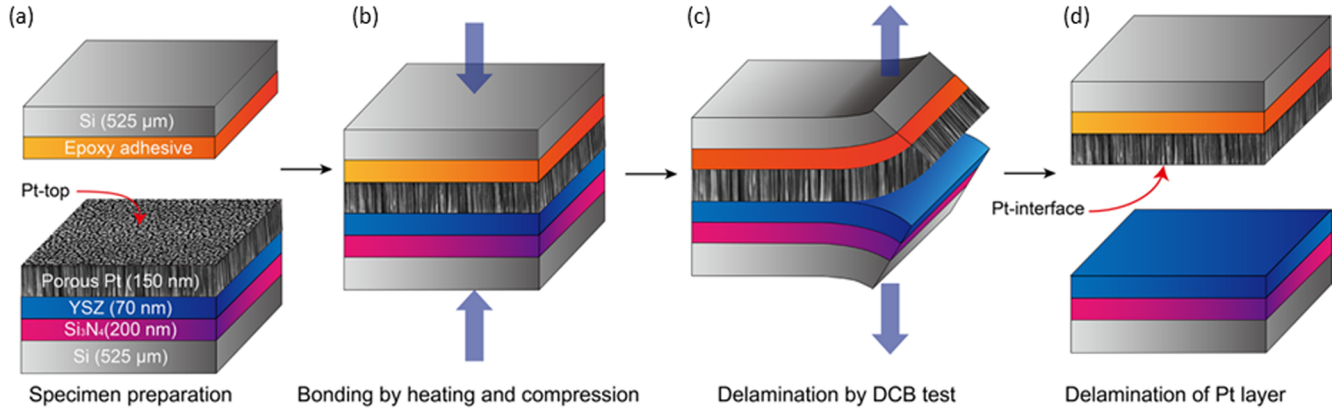

Figure 2. DCB delaminating process of nanoporous Pt from an YSZ substrate. (a) Porous Pt was deposited on YSZ; (b) dummy silicon strip with epoxy adhesive was bonded on Pt top surface; (c) delamination of porous Pt film from YSZ; (d) delaminated porous Pt film for interfacial observation.

DOI: 10.1021/acsami.5b00134
ACS Appl. Mater. Interfaces 2015, 7, 6036−6040

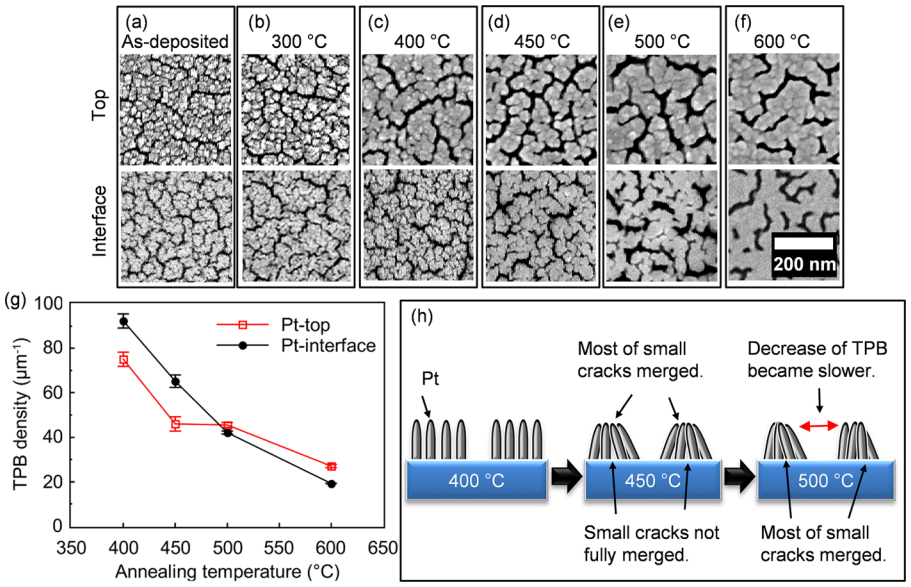

Figure 3. SEM images of the nanoporous Pt morphologies viewed from the top and interfacial perspectives for (a) as-deposited electrode, and (b–f) electrodes annealed at 300 to 600 °C. (g) TPB density as a function of annealing temperature by binary converted images method. (h) Illustration of Pt agglomeration at 400–500 °C.

the thermal agglomeration behaviors of the nanoscale pores between the Pt top view and Pt/YSZ contact interface are compared. The revealed interfacial TPB densities at various annealing temperatures are also compared with fuel cell performances using the annealed cathode.

Porous Pt films were deposited by DC magnetron sputtering on an YSZ thin film deposited on a silicon wafer (Figure 2a). After deposition, the porous Pt thin films were purposefully agglomerated via thermal annealing at 300, 400, 450, 500, and 600 °C in a tube furnace for 8 h. A dummy silicon strip with a thick layer of epoxy adhesive was bonded on to the porous Pt surface (Figure 2b), followed by delamination by a high precision micromechanical DCB test system (Figure 2c, d). The delamination is expected to occur at the Pt/YSZ interface rather than at YSZ/Si_3N_4 or Si_3N_4/Si interfaces because of the relatively weaker van der Waal bonding between Pt and YSZ. The delaminated surfaces on both the YSZ side and Pt side were examined and neither Pt residue on the YSZ surface nor YSZ residue on the Pt surface was found. The experimental details could be found in the Supporting Information, note S1.

The SEM images of the morphological evolution of porous Pt with increasing annealing temperature are shown in Figure 3. In the as-deposited Pt thin film (Figure 3a), a very high density of short, narrow, and nanometer-scale cracks exist between the larger, wider, and tens to hundreds of nanometers cracks. At 300 °C (Figure 3b), no apparent agglomeration was observed at both the top and interface because the temperature remained too low to activate the Pt migration. At 400 °C (Figure 3c), the agglomeration became noticeable as the cracks at both the top and interface merged and grew larger. As temperature increased, as expected, the pore morphology evolution differed significantly between the top and interface, particularly between 400 to 500 °C (Figure 3c–e). The smaller cracks inside Pt clusters on the top appeared to have completely merged at 400 °C, whereas those at the interface predominantly remained, and not until the temperature increased to 500 °C did the smaller cracks complete the merging. That is, the smaller cracks at the interface merged at 100 °C higher (500 °C) than those at the top surface (400 °C). This is due to the bonding force between the Pt and YSZ substrate that limits the mobility of the Pt particles so that the interfacial nanocracks is more resistant to thermal agglomeration, and the 100 °C of temperature difference value can be different if another electrolyte substrate with different wettability with Pt is used. As the temperature increased to 600 °C (Figure 3f), the cracks grew larger and wider both on the top and at the interface, and the morphologies were also similar without an apparent difference in TPB density. We estimated the variation of TPB density by counting the number of pixels on the TPB length with ImageJ software, as was the same method used by Wang et al.[11] The estimation of the as-deposited and 300 °C-annealed Pt were not shown here since the software were not able to accurately identified the TPB densities from very small cracks in the images. The results quantified and summarized the line densities of pore peripheral at all annealing temperatures (Figure 3g). Previously, Wang et al. also observed the nanoporous electrode agglomeration with various annealing temperatures, but only by viewing on the electrode "top view".[11] They concluded that the significant porosity drop due to the merger of the nanoscale pores began at 400 °C, which well agrees with our observations on the top surface. However, here from our interface observation results, a high density of nanoscale pores still remained at 400 °C to serve as effective TPBs. Even at a higher temperature of 450 °C, the pore densities at the interface were still higher than at the electrode top. The difference of the TPB density trend between Pt–top and Pt–interface can be explained as follows. As illustrated in Figure 3h, because the Pt–top surface was not constrained, the majority of the smaller cracks on the top surface will merged at lower temperature of 450 °C, which led to a significant drop in its TPB density. The TPB Pt–interface density remains high at 450 °C since the cracks were confined by the bonding to the substrate. As temperature increased from 450 to 500 °C, the majority of the smaller cracks at the Pt-interface merged significantly and the TPB continued to drop, whereas the TPB density decrease at Pt-top was less significant since the majority

DOI: 10.1021/acsami.5b00134
ACS Appl. Mater. Interfaces 2015, 7, 6036–6040

of the smaller cracks have already merged at lower temperatures. Only until the annealing temperature reached 500 °C and above, the TPB densities between the top and interface become similar. Without the observation of TPB density at the Pt/YSZ interface, one may try to keep the operating temperature of micro-SOFCs using nanoporous Pt electrode below 400 °C in order to avoid significant performance degradation from pore agglomeration. Here with our direct observation of TPB density at Pt/YSZ interface, one can opt to operate the cell at up to 500 °C without losing the contribution of TPBs from nanoscale pores significantly, and at the same time benefit from faster electrode kinetics at higher temperature.

We further characterized the annealed Pt thin films as SOFC cathodes by AC impedance spectroscopy to correlate their temperature-dependent performance with our morphological observation. These annealed cathodes were deposited on a ⟨100⟩ single-crystalline YSZ electrolyte substrate with sputtered porous Pt as the anode to form a single cell. The area specific resistance (ASR) of four cells with cathode Pt thin film as-deposited, annealed at 400, 500, and 600 °C is shown in Figure 4a. As expected, the ASR remained low before temperature

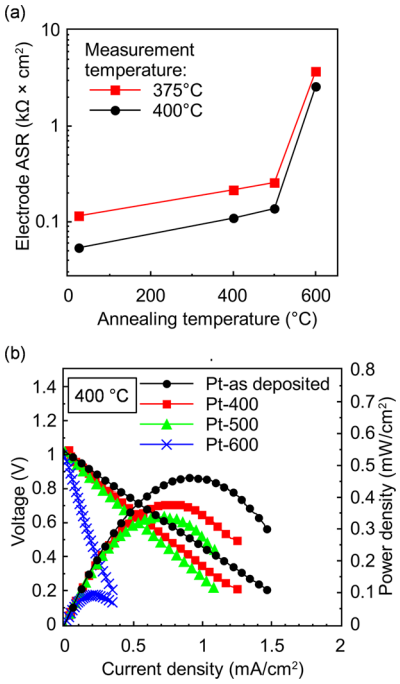

Figure 4. (a) Area specific resistance of as-deposited electrode and annealed electrodes. The results were measured at 375 and 400 °C. (b) Fuel cell performance of Pt cathode/YSZ/Pt anode single cell with cathode as-deposited, annealed at 400, 500, and 600 °C. The test was conducted at 400 °C, with pure H_2 as fuel and the cathode was open to ambient air.

reached 500 °C but increased significantly at 600 °C. The high ASR at 600 °C reflected the completed merging of nanoscale cracks that can no longer contribute to cathode ORR. The ASR at 500 °C is lower than expected, though, possibly because the merger of nanoscale cracks was not complete, and the nearly merged but invisible cracks still serve as effective TPB sites. The fuel cell polarization curves (Figure 4b) also exhibited only a small drop in performance from cathodes annealed at 400−500 °C but a significant drop from cathodes annealed at 500−600 °C. This also justified the cathode annealed at 500 °C and below remains a high density of nanoscale TPBs for higher device performance. The significant performance degradation from 500 to 600 °C might have been caused by the elimination of the invisible "nanoscopic" TPBs, as proposed by Ryll et al., being completed at 600 °C and caused a higher ASR of the electrode with the TPB density decrease.[10] By using the delamination technique in this study, the invisible nanoscopic TPBs and pores were identified to provide a better estimation of the TPB density with annealing temperature. Further identification of the geometrically nonmeasurable nanoscopic TPBs such as grain boundaries might be observed by combining the DCB delamination method with more advanced imaging techniques such as atomic force microscopy or scanning tunnelling microscopy.

In summary, the direct observations of the nanostructures at the Pt/YSZ contact interface were revealed by using the DCB method to delaminate the nanoporous Pt thin film from the YSZ substrate. Significant morphological differences between the Pt/YSZ interfaces were observed at annealing temperatures between 400 and 500 °C, and the nanoscale pores at the Pt/YSZ interface merged at 100 °C higher temperature that at the top surface, showing better thermal stability of nanoscale TPB pores at interface.

From the perspective of the crack dimensions, we propose the pore agglomeration occurs in two stages. The first stage occurs at temperatures at or below 500 °C, where the decrease in the TPB density results from the merging of the nanometer-sized smaller cracks. The second stage occurs as temperature is higher than 500 °C, where nanometer-sized cracks have merged completely, and the electrode agglomeration proceeded further through the merging of existing pores into tens to hundreds of nanometers size. To retain the thermal stability of μ-SOFCs using a nanoporous electrode without significant degradation of cell performance, the operating temperatures can be higher than 400 °C but below 500 °C.

■ ASSOCIATED CONTENT

Supporting Information

Experimental details including sample preparation, delamination, image process, electrochemical impedance spectroscopy measurement, and fuel cell characterization. This material is available free of charge via the Internet at http://pubs.acs.org.

■ AUTHOR INFORMATION

Corresponding Authors

*E-mail: peichensu@ntu.edu.sg.
*E-mail: tskim1@kaist.ac.kr.

Author Contributions

†Authors C.C.Y. and S.K. contributed equally to this work. The manuscript was written through contributions of all authors. C.C.Y. and S.K. performed experiment and analysis. Y.L., J.D.B., P.C.S., and T.S.K. served in an advisory capacity. All authors have given approval to the final version of the manuscript.

Funding

MOE Tier 1 Grant (RG 92/13) from Singapore Ministry of Education, Singapore NRF-2011-0031569 and NRF-2012R1A1A1006072 from National Research Foundation of Korea, Republic of Korea

Notes

The authors declare no competing financial interest.

DOI: 10.1021/acsami.5b00134
ACS Appl. Mater. Interfaces 2015, 7, 6036−6040

■ ACKNOWLEDGMENTS

The authors acknowledge the financial support from MOE Tier 1 Grant (RG 92/13) from Singapore Ministry of Education and from the National Research Foundation of Korea (NRF-2011-0031569, NRF-2012R1A1A1006072).

■ ABBREVIATIONS

YSZ, yttria-stabilized zirconia
TPB, triple phase boundary
ORR, oxygen reduction reaction
μ-SOFCs, micro solid oxide fuel cells
DCB, double cantilever beam
ALD, atomic layer deposition
PVD, physical vapor deposition
CPE, constant phase element
ASR, area specific resistances

■ REFERENCES

(1) Kloke, A.; von Stetten, F.; Zengerle, R.; Kerzenmacher, S. Strategies for the Fabrication of Porous Platinum Electrodes. *Adv. Mater.* **2011**, *23*, 4976−5008.
(2) Su, P.-C.; Prinz, F. B. Nanoscale Membrane Electrolyte Array for Solid Oxide Fuel Cells. *Electrochem. Commun.* **2012**, *16*, 77−79.
(3) Huang, H.; Nakamura, M.; Su, P.; Fasching, R.; Saito, Y.; Prinz, F. B. High-Performance Ultrathin Solid Oxide Fuel Cells for Low-Temperature Operation. *J. Electrochem. Soc.* **2007**, *154*, B20−B24.
(4) Su, P. C.; Chao, C. C.; Shim, J. H.; Fasching, R.; Prinz, F. B. Solid Oxide Fuel Cell with Corrugated Thin Film Electrolyte. *Nano Lett.* **2008**, *8*, 2289−2292.
(5) An, J.; Kim, Y. B.; Park, J.; Gur, T. M.; Prinz, F. B. Three-Dimensional Nanostructured Bilayer Solid Oxide Fuel Cell with 1.3 W/cm(2) at 450 °C. *Nano Lett.* **2013**, *13*, 4551−4555.
(6) Adler, S. B. Factors Governing Oxygen Reduction in Solid Oxide Fuel Cell Cathodes. *Chem. Rev.* **2004**, *104*, 4791−4843.
(7) Guenther, K. H. Revisiting Structure-Zone Models for Thin-Film Growth. *Proc. SPIE* **1990**, *1324*, 2−12.
(8) Kerman, K.; Lai, B. K.; Ramanathan, S. Pt/Y0.16Zr0.84O1.92/Pt Thin Film Solid Oxide Fuel Cells: Electrode Microstructure and Stability Considerations. *J. Power Sources* **2011**, *196*, 2608−2614.
(9) Radhakrishnan, R.; Virkar, A. V.; Singhal, S. C. Estimation of Charge-Transfer Resistivity of Pt Cathode on YSZ Electrolyte Using Patterned Electrodes. *J. Electrochem. Soc.* **2005**, *152*, A927−A936.
(10) Ryll, T.; Galinski, H.; Schlagenhauf, L.; Elser, P.; Rupp, J. L.; Bieberle-Hutter, A.; Gauckler, L. J. Microscopic and Nanoscopic Three-Phase-Boundaries of Platinum Thin-Film Electrodes on YSZ Electrolyte. *Adv. Funct. Mater.* **2011**, *21*, 565−572.
(11) Wang, X. H.; Huang, H.; Holme, T.; Tian, X.; Prinz, F. B. Thermal Stabilities of Nanoporous Metallic Electrodes at Elevated Temperatures. *J. Power Sources* **2008**, *175*, 75−81.
(12) Simrick, N. J.; Kilner, J. A.; Atkinson, A. Thermal Stability of Silver Thin Films on Zirconia Substrates. *Thin Solid Films* **2012**, *520*, 2855−2867.
(13) Galinski, H.; Ryll, T.; Elser, P.; Rupp, J. L. M.; Bieberle-Hütter, A.; Gauckler, L. J. Agglomeration of Pt Thin Films on Dielectric Substrates. *Phys. Rev. B* **2010**, *82*, 235415.
(14) Dupont, S. R.; Voroshazi, E.; Heremans, P.; Dauskardt, R. H. Adhesion Properties of Inverted Polymer Solar Cells: Processing and Film Structure Parameters. *Org. Electron.* **2013**, *14*, 1262−1270.
(15) Yoon, T.; Shin, W. C.; Kim, T. Y.; Mun, J. H.; Kim, T. S.; Cho, B. J. Direct Measurement of Adhesion Energy of Monolayer Graphene As-Grown on Copper and Its Application to Renewable Transfer Process. *Nano Lett.* **2012**, *12*, 1448−1452.

DOI: 10.1021/acsami.5b00134
ACS Appl. Mater. Interfaces 2015, 7, 6036−6040